AD-A106 031 MISSION RESEARCH CORP LA JOLLA CA F/G 17/7
CHARACTERIZATION OF THE RADIATION HARD HARRIS/DINS RING LASER G--ETC(U)
JUN 80 B C PASSENHEIM DNA001-80-C-0140
UNCLASSIFIED MRC/SD-R-57 DNA-5351T NL

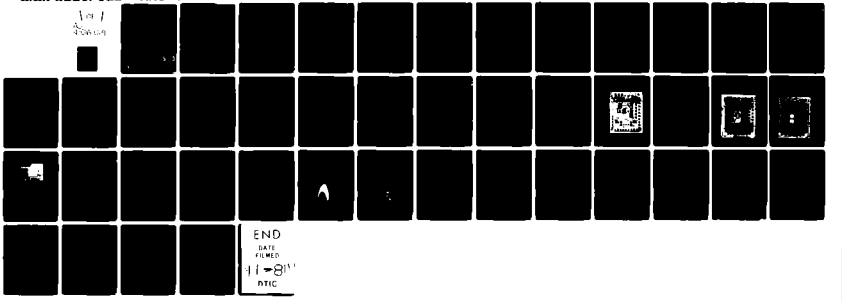

END
DATE FILMED
11-81
DTIC

LEVEL I

DNA 5351T

AD A106031

CHARACTERIZATION OF THE RADIATION HARD HARRIS/DINS RING LASER GYRO PHOTODETECTORS

Burr C. Passenheim

Mission Research Corporation
P.O. Box 1209
La Jolla, California 92038

30 June 1980

Topical Report for Period 28 January 1980—30 June 1980

CONTRACT No. DNA 001-80-C-0140

APPROVED FOR PUBLIC RELEASE;
DISTRIBUTION UNLIMITED.

THIS WORK SPONSORED BY THE DEFENSE NUCLEAR AGENCY
UNDER RDT&E RMSS CODE B323080464 X99QAXVB20102 H2590D.

Prepared for
Director
DEFENSE NUCLEAR AGENCY
Washington, D. C. 20305

Destroy this report when it is no longer needed. Do not return to sender.

PLEASE NOTIFY THE DEFENSE NUCLEAR AGENCY, ATTN: STTI, WASHINGTON, D.C. 20305, IF YOUR ADDRESS IS INCORRECT, IF YOU WISH TO BE DELETED FROM THE DISTRIBUTION LIST, OR IF THE ADDRESSEE IS NO LONGER EMPLOYED BY YOUR ORGANIZATION.

UNCLASSIFIED

SECURITY CLASSIFICATION OF THIS PAGE (When Data Entered)

REPORT DOCUMENTATION PAGE

READ INSTRUCTIONS BEFORE COMPLETING FORM

1. REPORT NUMBER: DNA 5351T	2. GOVT ACCESSION NO.: AD-A106 083
3. RECIPIENT'S CATALOG NUMBER:	
4. TITLE (and Subtitle): CHARACTERIZATION OF THE RADIATION HARD HARRIS/DINS RING LASER GYRO PHOTODETECTORS.	5. TYPE OF REPORT & PERIOD COVERED: Topical Report for period 28Jan80 — 30Jun80
	6. PERFORMING ORG. REPORT NUMBER: MRC/SD-R-57
7. AUTHOR(s): Burr C. Passenheim	8. CONTRACT OR GRANT NUMBER(s): DNA 001-80-C-0140
9. PERFORMING ORGANIZATION NAME AND ADDRESS: Mission Research Corporation, P.O. Box 1209, La Jolla, California 92038	10. PROGRAM ELEMENT, PROJECT, TASK AREA & WORK UNIT NUMBERS: Subtask X99QAXVB201-02
11. CONTROLLING OFFICE NAME AND ADDRESS: Director, Defense Nuclear Agency, Washington, D.C. 20305	12. REPORT DATE: 30 June 1980
	13. NUMBER OF PAGES: 42
14. MONITORING AGENCY NAME & ADDRESS (if different from Controlling Office)	15. SECURITY CLASS (of this report): UNCLASSIFIED
	15a. DECLASSIFICATION DOWNGRADING SCHEDULE: N/A

16. DISTRIBUTION STATEMENT (of this Report)

Approved for public release; distribution unlimited.

17. DISTRIBUTION STATEMENT (of the abstract entered in Block 20, if different from Report)

18. SUPPLEMENTARY NOTES

This work sponsored by the Defense Nuclear Agency under RDT&E RMSS Code B323080464 X99QAXVB20102 H2590D.

19. KEY WORDS (Continue on reverse side if necessary and identify by block number)

Optical photocurrents
Radiation photocurrents
Photodiodes
Photodetectors
Responsivity
Antireflection coating
Dielectric isolation
Ring laser gyro
Dormant inertial navigation system

20. ABSTRACT (Continue on reverse side if necessary and identify by block number)

Specially designed radiation hard dielectrically isolated photodiodes constructed specifically for a HeNe (632.8 nm) ring laser gyroscope, have been characterized. The spectral response shows a peak of 0.4 ± 0.1 A/watt in the range of 600 to 700 nm. The measured radiation induced photocurrent of $5.7 \pm 1.8 \times 10^{-13}$ coul/rad compares favorably with expectations based on device geometry (7.8×10^{-13} coul/rad). Under nominally identical illumination, optical photocurrents from matching detectors agree to approximately

(continued)

DD FORM 1 JAN 73 1473 EDITION OF 1 NOV 65 IS OBSOLETE

UNCLASSIFIED

SECURITY CLASSIFICATION OF THIS PAGE (When Data Entered)

20. (continued)

1.5 ± 0.5 percent and ionizing radiation produced photocurrent agrees to approximately 6 ± 4 percent. Detectors which had been exposed to ~~10^6~~ million rad(Si) exhibited responsivities 78 ± 14 percent as large as that of virgin detectors. Chip to chip responsitivity variations were about ± 30 percent. Relevant physics and construction details are reported.

PREFACE

The photodiodes described in this report were designed under contracts DNA001-77-C-0174 and DNA001-78-C-0050. The photodiodes were constructed under contract DNA001-78-C-0356 and were tested under contract number DNA001-80-C-0140. These devices were designed, constructed, and tested to support the development by the USAF (Advanced Ballistic Re-entry System and Ballistic Missile Office) of a dormant inertial navigation system (DINS), employing laser gyroscopes.

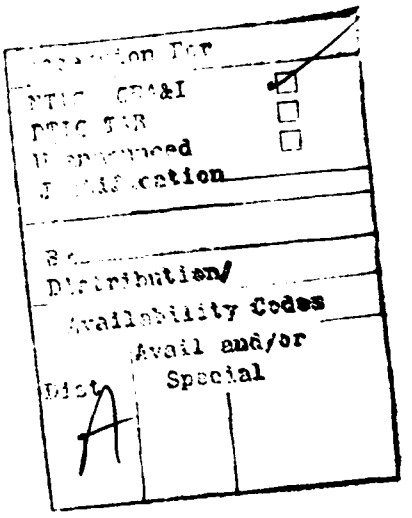

TABLE OF CONTENTS

LIST OF ILLUSTRATIONS

LIST OF ILLUSTRATIONS (Continued)

1. INTRODUCTION

This report documents the characterization of the Harris/DINS photodetectors in optical and ionizing radiation. Section 2 is a historical review of the events which proceed construction and testing of these diodes. Section 3 reviews the relevant physics involved in the design and construction of these devices. Section 4 describes the actual steps employed to construct the devices and provides the results of a visual examination. Section 5 describes these tests and presents the relevant results.

2. HISTORICAL REVIEW

In late 1976 the Air Force decided to examine the ring laser gyroscope constructed by Honeywell Incorporated as a candidate for a re-entry vehicle guidance system called the dormant inertial navagation system (DINS).

Under Defense Nuclear Agency sponsorship, the nuclear survivability and vulnerability (S & V) of the laser block assembly and associated electronics was examined theoretically and tested experimentally between February and September of 1977. At the time of this initial investigation, Honeywell was using a commercially available photodetector (United Detector Technology's PIN-SPOT-2) to detect the motion of the interference fringes which indicate rate and direction of gyro rotation.

Our initial evaluation, which was supported by subsequent measurements, was that for this laser/detector combination the optical radiation photocurrents would be exceeded by ionizing radiation photocurrents, whenever the dose rate exceeded 10^2 rads(Si)/s. An error analysis indicated that laser gyro operations could be interrupted by a transient radiation event for no more than approximately 1 millisecond. Relating this to a hypothesized nuclear event caused us to select a dose rate of 10^7 rads(Si)/s as an operational design goal. At that time we found there were no commercially available photodiodes which could even approach that goal. In fact the signal to noise (S/N) ratio of event the most radiation tolerate photodiodes fell below unity at rates of approximately 3×10^3 rads/s.

This was only a consequence of the designs then available. It was not a technology limitation, and so by September 1977, we concluded that, although there were no commercially available substitutes, it was technically feasible to build a DINS-specific photodiode, optimized for use with the ring laser gyro, in a radiation environment.[1,2] The reasons for the specific design are presented in Section 3 and the details of the construction are presented in Section 4. This design is related to work reported by Mitchell[3] and photodiodes designed for AFWL for fiberoptics applications, by Arnie Kalma and Walt Hardwick, which have since been constructed by Spectronics. The specific design for the radiation hard DINS photodiode was given to the Defense Nuclear Agency in December 1977. This design was a compromise, using proven, high confidence, existing technology techniques, optimized to result in a photodetector which would operate with a signal noise ratio in excess of unity at dose rates of 10^7 rads(Si)/s ($\sim 10^5$ x higher than was possible in 1977).

Several device manufacturers were asked to construct the DINS diodes. Only Harris responded affirmatively. The proposed design for the photodiode was supplied to Jon Cornell of Harris Semiconductor in January of 1978. A technical meeting was held at Harris Semiconductor in February of 1978 attended by the Defense Nuclear Agency representatives. The

proposal resulting from that meeting was dated June 1978 and the first generating of parts was supplied by Harris Semiconductor to Honeywell for testing approximately one year later. The first generation of DINS photodiodes were tested in July of 1979. That generation of chips had several geometry design variations and two doping density variations.[4] There was no significant performance difference among the various geometry variations. Some of the doping variations exhibited poor electrical characteristics (specifically ~10 percent of the diodes were shortened) and only a few of the diodes approached the desired 1 percent photocurrent matching. Exact photocurrent matching was desired because we intended to illuminate only one of a pair of identical photodiodes supplying signals to a differential amplifier (see Figure 1). Thus the (common mode) ionizing radiation photocurrent I_γ (considered to be CW noise) from the blind diode would be subtracted from the (differential) optical signal plus (common mode) noise from the sighted diode. Our ability to cancel noise depends on diode matching and common mode rejection ratio of the amplifier.

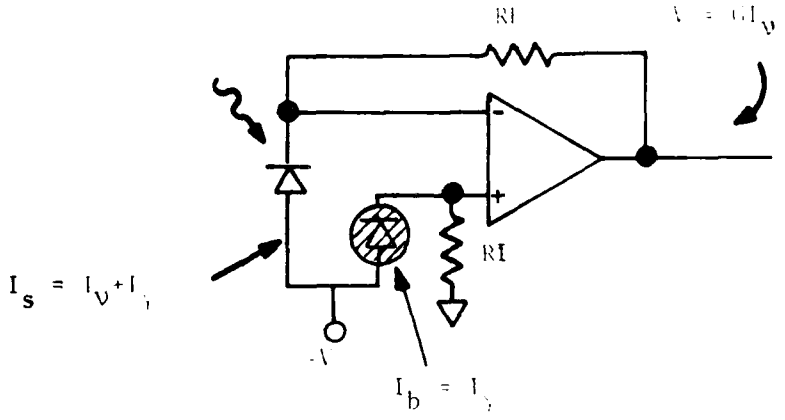

Figure 1. Use of a blind diode and a differential amplifier to subtract radiation noise from the optical signal.

In fact, a small but constant photocurrent mismatch in the diode pair could be tolerated if RF or RI were adjusted to compensate for this mismatch. Unfortunately we noted that photocurrent mismatch was a function of total accumulated dose. In particular if $I_b = 1.05\ I_s$ before irradiation $I_b = I_s$ about 50 K rad and $I_b = 0.85\ I_s$ at 100 to 200 K rad. (I_b is blind diode photo current I_s sighted photodiode current).

The results of the optical and radiation tests were provided to Harris Semiconductor in August of 1979 and Harris set about to construct a second generation of test chips. The second generation of test chips used a different metalization pattern than the first. Also, Harris reported they had experienced wafer processing problems with the first generation and chose to fabricate new wafers for the second generation of device. The second generation of photodiodes was provided to Honeywell in early 1980 and was tested by MRC in May 1980.

3. Relevant Physics

Carrier generation by ionizing radiation results in radiation photocurrents that can temporarily obscure the optical photocurrent. Carrier removal and lifetime degredation permanently alter the collection volume by increasing the depletion depth and decreasing the diffusion length in the bulk material.

Photodiodes, phototransistors, and solar cells are designed to have maximum sensitivity to optical radiation. For maximum efficiency and ease of construction, photodetectors are frequently much thicker than $[\alpha(\lambda)]^{-1}$, the optical absorption absorption depth at wavelength λ (632.8 nm in this case). The bulk material usually has a long lifetime to obtain a maximum collection efficiency for minority carriers. Generally, the same features that make a good photodetector also make the device very sensitive to all nuclear radiation.

The responsivity (amps/watt) of a planar photodetector is given by

$$I_\nu/HA = \frac{nq}{h\nu}\ (1\text{-}R)\ h\nu > 1.1\ eV \qquad (1)$$

where I_ν is the photocurrent
H is the irradiance (watts/cm^2)
A is the detector area
η_i is the collection efficiency
$\frac{nq}{h\nu}$ is the photoelectric charge generated per photon
$h\nu$ is the photo energy, and
R is reflectance.

The quantity $q/h\nu$ is the maximum responsivity possible (0.509 A/watt) at 632.8 nm. The coefficient η_i represents the optical collection efficiency, $\eta_i \simeq 1 - \exp[-\alpha(L+W)]$ where α is the optical absorption coefficent, L is the diffusion length, and W is the depletion width. The optical absorption coefficient for silicon is given in Figure 2. At 632.8 nm, $\alpha_{Si}(632.8\ nm) = 3{,}600\ cm^{-1}$ so $\alpha^{-1}(632.8\ nm) = 2.8\ \mu m$. The collection efficiency expresses two facts. First, the number of optically generated photocarriers decreases exponentially with distance from the front surface, and second that only carriers that are generated within the depletion width (W) and/or within a diffusion length (L) of the junction edge will supply current to an external circuit. Carriers generated deeper in the bulk material will recombine before they can contribute current to an external circuit. But, if $(L+W) > [\alpha(\lambda)]^{-1}$ radiation induced photocurrents can be generated and collected from depths which contibute nearly no optical photocurrents.

When a photodetector is exposed to penetrating radiation, such as silicon-prefiltered light, x-rays or gamma-rays, the radiation photocurrent can be described by

$$I_\gamma/\dot{D} = gAq(W+L) \qquad (2)$$

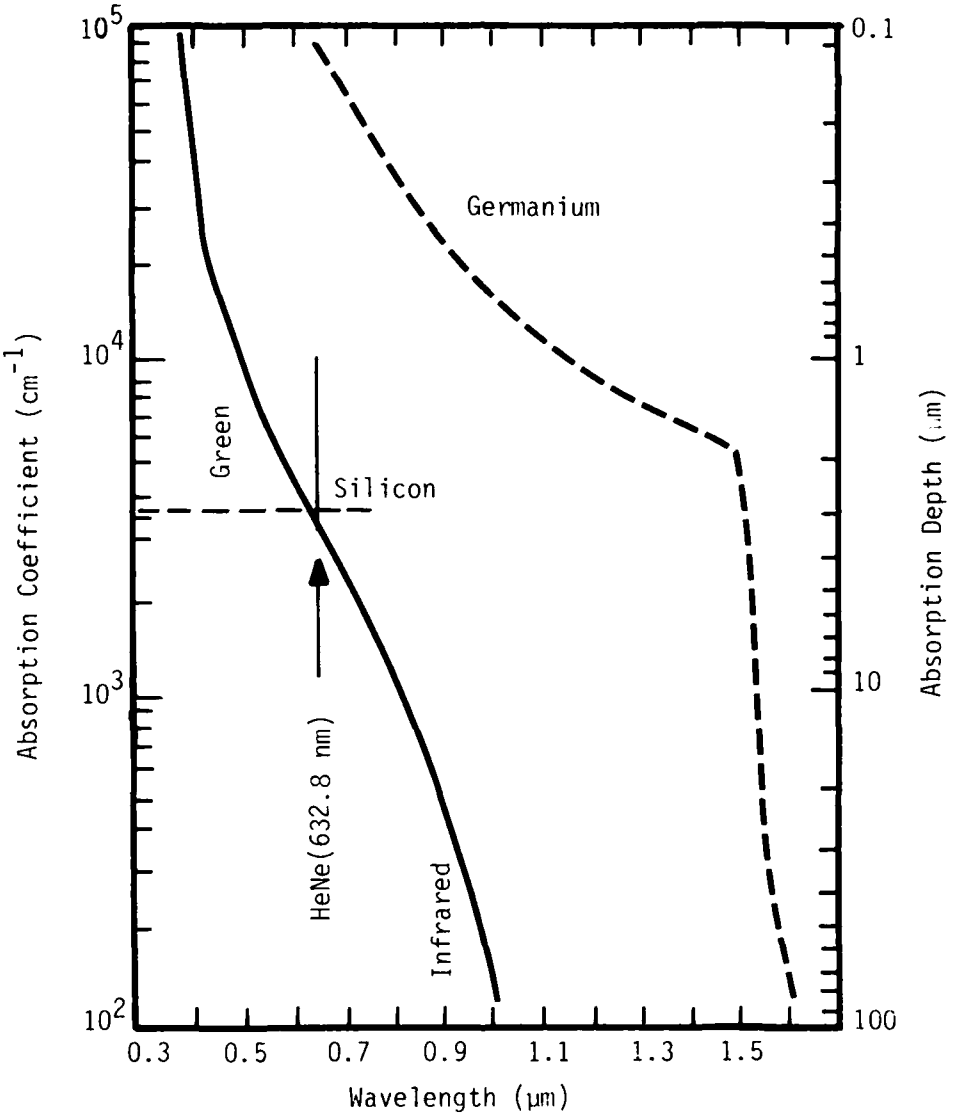

Figure 2. Absorption coefficient (left) or absorption depth (right) vs. wavelength for silicon and germanium at room temperature (Dash and Newman).

where $\dot{D}$ is the dose rate, q is the electronic charge and g, the generation rate for silicon, is $\sim 4 \times 10^{13}$ carriers/cm^3 rad. For silicon,

$$I_\gamma/\dot{D} \approx 6.4 \times 10^{-6} \frac{\text{A-sec}}{\text{rad cm}^3} \times A(L+W).$$

It has been shown in Reference 3 that the ratio of optical to radiation photocurrents at 632.8 nm continues to increase as L+W decreased, however, the total optical photocurrent, for a given irradiance decreases as L+W gets less than a few absorption layers thick.

The most important factor is that optical photocurrents of 632.8 nm light are all generated within the first few micrometers of silicon surface, whereas radiation photocurrents are generated throughout the depletion volume, (detector area (A) times depletion width (W)). For lightly doped diodes, with planar geometry, depletion width (W) is related to bias voltage V as

$$W = \sqrt{2\varepsilon\varepsilon_o V/qN}$$

where $\varepsilon = 13$ for silicon, $\varepsilon_o = 8.85 \times 10^{-14}$ Farads/cm, $q = 1.6 \times 10^{-19}$ coulombs and N is the doping density. Doping density is inferred from material resistivity $\rho = (q(N_e\mu_e + N_h\mu_h))^{-1}$ where $\mu_e = 1300$ cm^2/Vs and $\mu_h = 450$ cm^2/Vs. In the field-free bulk region, the minority carrier lifetime (τ_D) and the diffusion length (L) are related by

$$\tau_D = L^2/D$$

where D is the diffusion constant (33 cm^2/s for electrons and 11 cm^2/s for holes in silicon).

Hense the ratio of optical currents to radiation photocurrents depends upon detector geometry as (from equations 1 and 2)

$$\frac{I_\nu}{I_\gamma} \approx \frac{\{1- \exp\ [-\alpha(L+W)\ ]\}\ (1-R)}{h\nu g(L+W)} \approx (S/N)$$

From a practical point of view, you want to maximize both the signal and the signal/noise ratio (I_ν^2/I_γ). The product of optical photocurrent times signal/noise ratio has a broad maximum when $L+W \approx 1.5\ [\alpha(\lambda)\ ]^{-1}$. This was the reason for the design goal presented to Harris Semiconductor, to construct diodes approximately 5 μm thick.

An added bonus is that a very thin detector becomes quite neutron and total dose tolerant as well, since the lifetime τ must be reduced to approximately the sweep-out time τ_s before carrier recombination causes loss in detector sensitivity. Sweep-out time is $\tau_s = W^2/2\ \mu V$, where μ is mobility (μ_e = 1300 cm^2/s, μ_h = 450 cm^2/s in silicon). For the designed geometry ($W < 5 \times 10^{-4}$ cm) and bias voltages ($V \approx 10v$) $\tau_s \approx 10^{-10}$ s. Lifetime is decreased by neutron radiation according to the formula $1/\tau = 1/\tau_o + K(\rho)\Phi$ where the lifetime damage constant $K(\rho)$ is shown in Figure 3. Since $\tau_o \approx 10^{-6}$ s, and $\tau_s << \tau_o$ we don't expect detection degradation at neutron fluences of less than about

$$\phi = (K\tau_s)^{-1} \approx 2 \times 10^{15} n/cm^2$$

which is well above our design guideline.

The lateral geometry of the photodetector was selected somewhat arbitrarily. The laser gyro's output beam, with its interference pattern, is nominally 1 mm in diameter. This author judged that it would be easy to reduce that pattern by a factor of 4, to a ¼ mm (0.010") diameter and that positioning a ¼ mm detector with a 1 mm diameter reducing lens within the 1 mm diameter interface pattern would not be unduely difficult.

4. CONSTRUCTION

Figure 4 schematically indicates the processing steps Harris used to create the 5 μm thick detectors. In step #1 they took a 20-mil (500 μm)

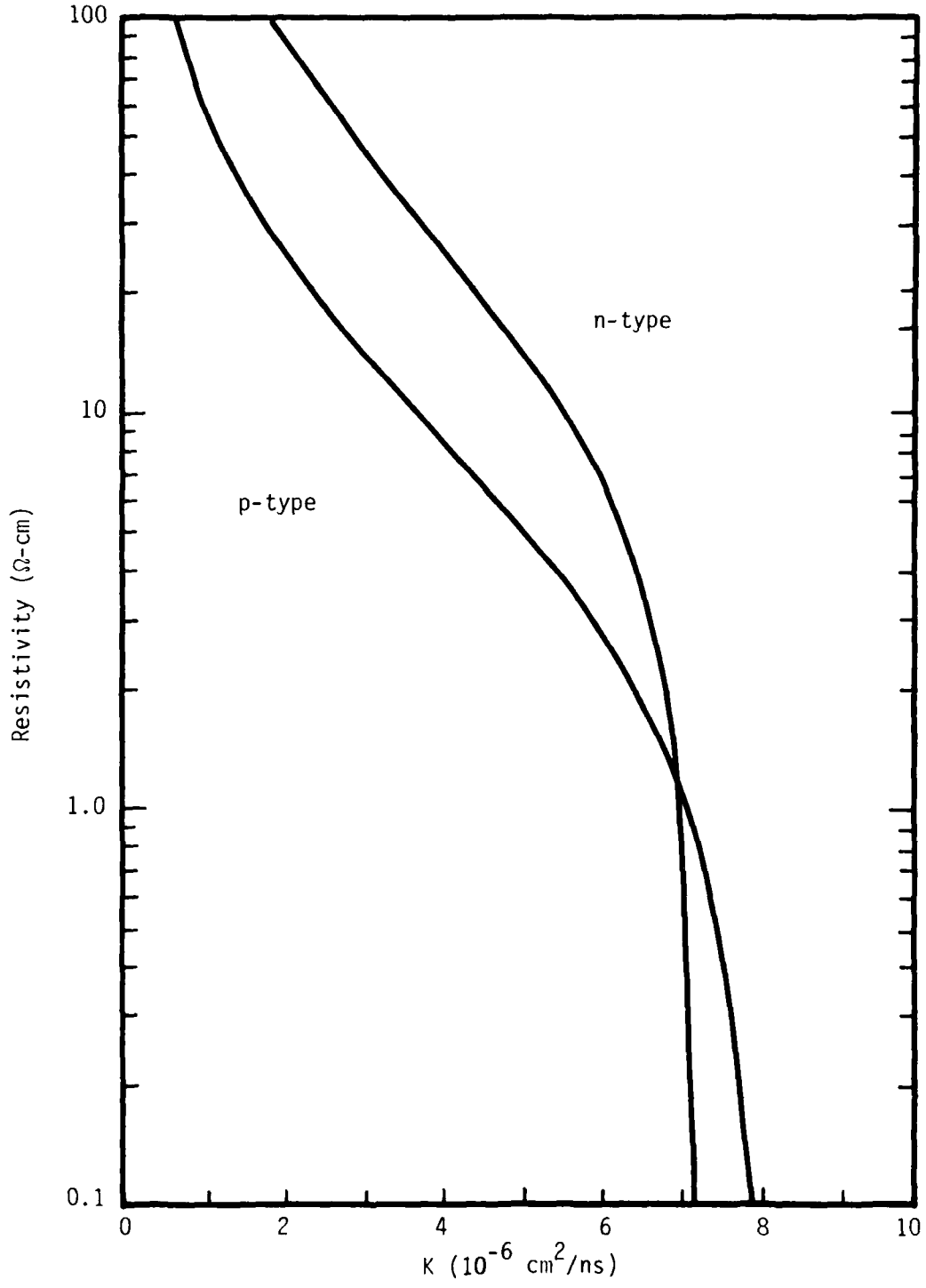

Figure 3. Lifetime damage constant versus resistivity for silicon at very low injection ($\Delta n/n_0 \sim 10^{-4}$). (At normal operating currents in transistors the damage constant may be less by a factor of 5 to 10.)

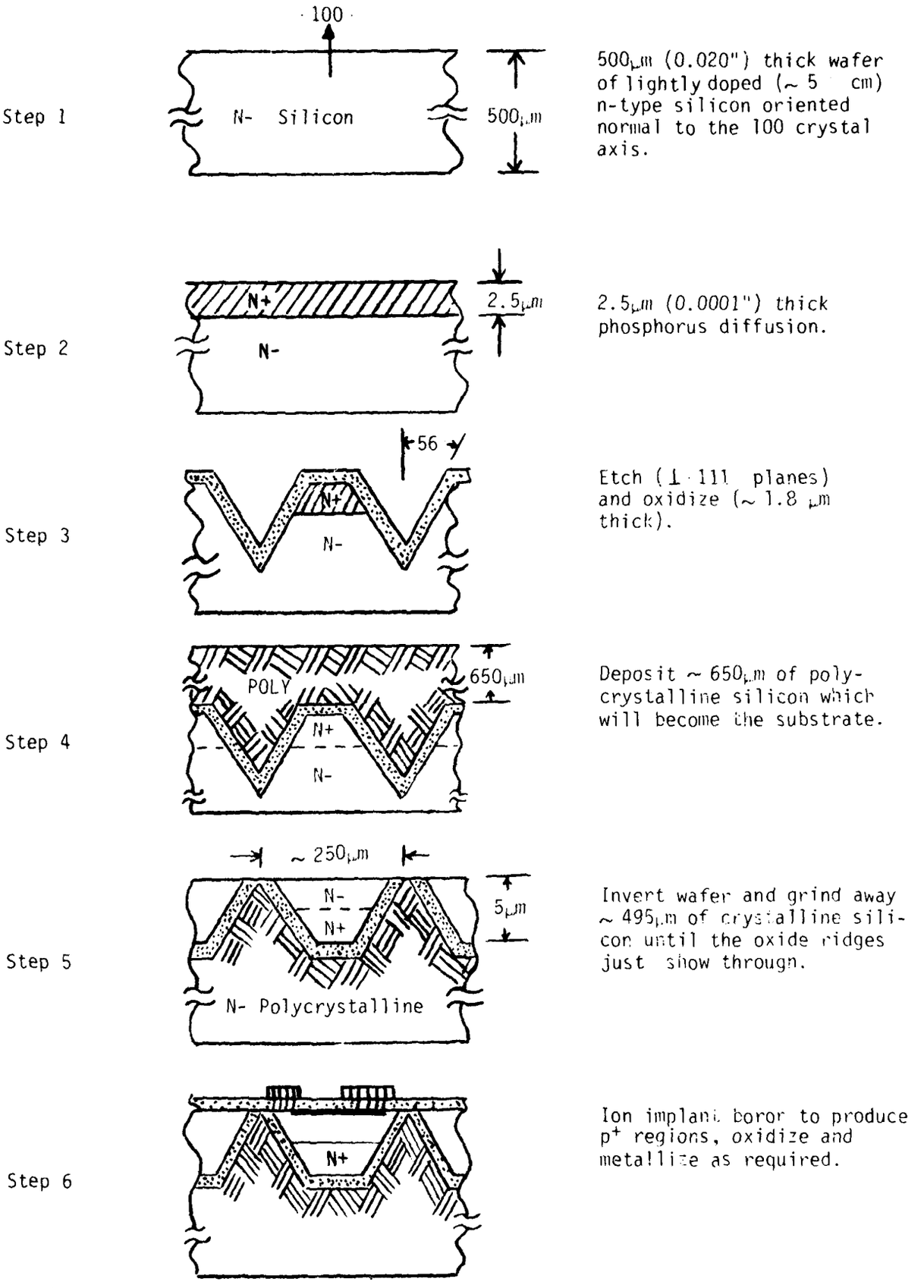

Step 1

500μm (0.020") thick wafer of lightly doped (~ 5 cm) n-type silicon oriented normal to the 100 crystal axis.

Step 2

2.5μm (0.0001") thick phosphorus diffusion.

Step 3

Etch (⊥ 111 planes) and oxidize (~ 1.8 μm thick).

Step 4

Deposit ~ 650μm of polycrystalline silicon which will become the substrate.

Step 5

Invert wafer and grind away ~ 495μm of crystalline silicon until the oxide ridges just show through.

Step 6

Ion implant boron to produce p^+ regions, oxidize and metallize as required.

Figure 4. Summary of processing steps to produce radiation hard dielectrically isolated photodetectors.

thick slab of lightly doped (3-6Ω cm) crystalline silicon cut normal to the 100 axis. In step #2 phosphorus was diffused about 0.0001" (2.5 μm) into the n crystalline silicon to form a thin n^+ phosphorus doped region. Then in step #3 the crystalline silicon was masked, etched, and oxidized to form a series of oxide covered mesas which later became the dielectric tubs which define the device geometry. In step #4 polycrystalline silicon was deposited on top of the oxidized crystalline substrate, then in Step #5 the polysilicon became the device substrate and the crystalline material was ground away to form thin (0.0002") devices. Finally, the p^+ front contact was produced by a boron implantation technique. The final detectors were semi circles 10 mils in diameter separated by about 0.5 mil and contained in a 0.2 mil thick dielectric tub.

The final oxidation was controlled in an effort to produce an antireflecting layer of thickness $t = (2N + 1)\ \lambda/4n$ where N is an integer, n is the index of refraction of the coating and λ is 632.8 nm. Both oxide and nitride A.R. coating were tried.

The reflectance at a single interface between a media with index of refraction n_o and one with n, is $R = (n-n_o/n+n_o)^2 = 30\%$ for silicon. For a single layer filter the reflectance is

$$R = \left[\frac{n_1^2 - n_o n_2}{n_1^2 + n_o n_2}\right]^2 \qquad (3)$$

where for air, $n_o \approx 1.0$, for silicon at 632.8 nm $n_2 = \sqrt{13} = 3.68$, for SiO_2 $n_1 \approx 1.5$ and Si_3N_4 $n_1 \approx 2.0$. Notice the <u>ideal</u> single layer filter at normal incidence would have an index of refraction $n_1 = (\varepsilon\varepsilon_o)^{\frac{1}{4}} = 1.899$ and thickness t = 833 nm (or 250 nm, or 416 nm etc.).

From equation 3, the best one can expect for SiO_2 (n = 1.5) is about a 6 percent loss due to reflection if t = 110 nm, while a 80 nm

thick layer of Si_3N_4 gives only a 0.16 percent loss. Conversely, the worst one can do, is deposit a layer of thickness $t = \lambda/2n$ which would result in a SiO_2 coating with only 85 percent transmission and on Si_3N_4 coating which transmitts 72 percent. Either case is an improvement over uncoated silicon.

Harris considered a two layer AR coating of SiO_2 and Si_3N_4 and concluded that it was more reflective than, i.e. not as good as, a single layer coating. We note this is apparently in contradiction with the findings of solar cell manufacturers.[6,7,8] However, it is this authors opinion that a properly deposited single layer AR coating of either SiO_2 or Si_3N_4 would be satisfactory, and that the potential of an additional 1 to 2 percent improvement from a "perfect" AR coating doesn't warrant a significant effort. The potential for error and/or device degradation increases with each successive process, and better results almost always are obtained from familiar actions, i.e. SiO_2 is preferable to less frequently used materials. Consequently this author agrees with Harris' conclusion that the best AR coating is a single $\lambda/4$ layer of SiO_2 or Si_3N_4 (albiet for different reasons).

When this design was originally proposed, the lens for reducing the interface pattern was not defined. Since then, Honeywell has selected an immersion lens concept, schematically indicated in Figure 5. In this design the thick plano-convex lens is cemented directly to the chip with an optical cement. This means the single layer SiO_2 or Si_3N_4 AR coating, which was optimized for an air-silicon interface is no longer the best.

Although this may represent an unwarranted nicety, the proper design would now be a $\lambda/4$ layer of material with $n \approx \sqrt{n_{SiO_2}}$ (MgF_2 perhaps) on the front surface of the lens (to reduce the 4 percent reflection at that interface) and another $\lambda/4$ layer of material with index of refraction $n = \sqrt{n_{SiO_2}\, n_{Si}}$ on the detector to reduce the reflection at the lens

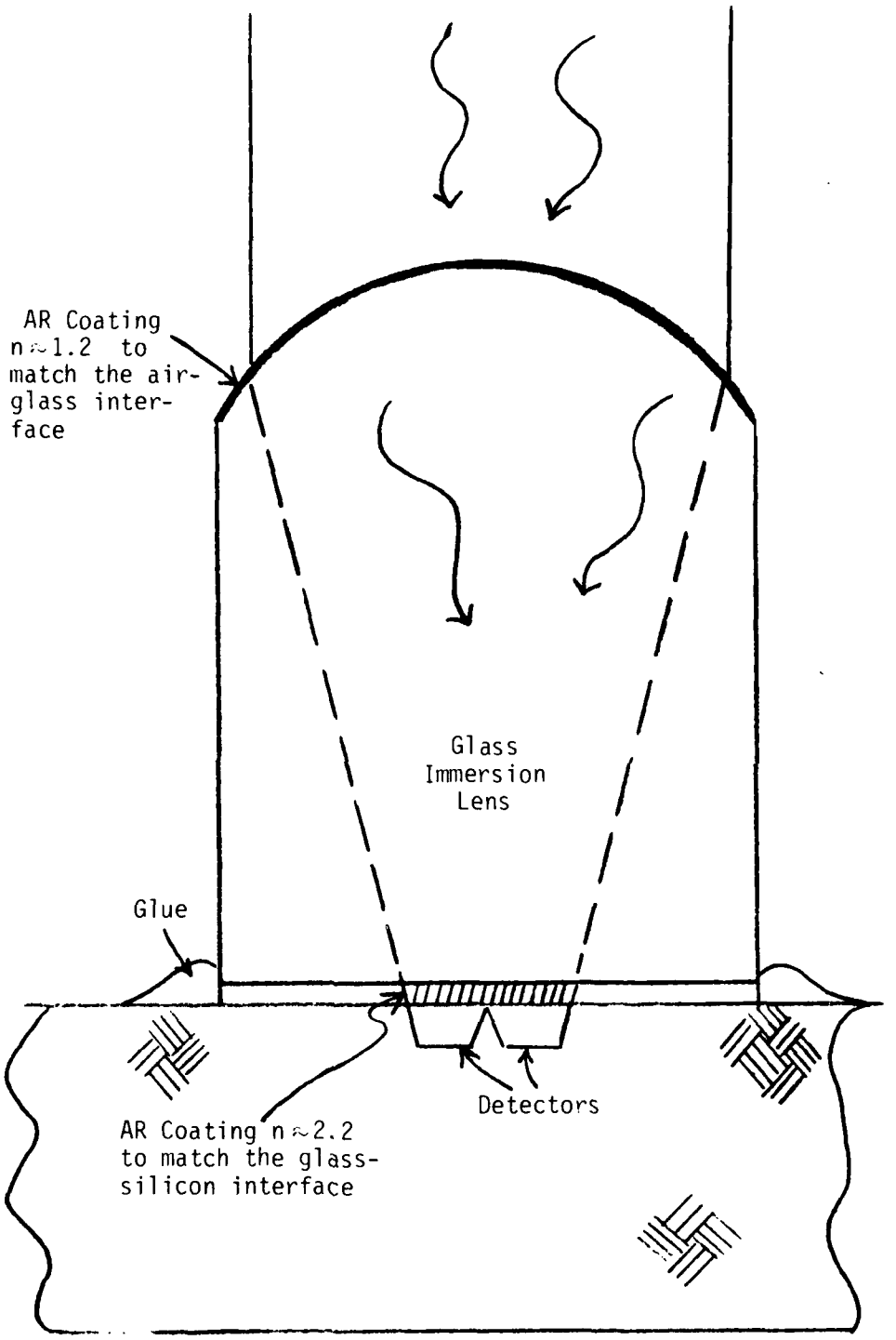

Figure 5. Schematic cross section of a dielectrically isolated photodiode pair, with glass immersion lens and AR coating.

detector interface. Titanium oxide, TiO_x, n = 2.2 or tantalum oxide, Ta_2O_5 with n = 2.2 ± 0.05 are good candidates. Finally, it is theoretically feasible (though unnecessary for this application) to make even more radiation tolerant photodiodes, without sacrificing 632.8 nm responsivity by 1) making the diodes still thinner, 2) further reducing their lateral dimensions and 3) encapsulating them in a reflective tub. This could (theoretically) be accomplished with a thin (≈ 0.1 μm) evaporated aluminum layer between the oxide of the tub and the polycrystalline substrate, or by controlling the oxide thickness to produce a dielectric mirror. Both these concepts were known to this author when the original design was proposed in 1977-78. However, they were not proselytized because they were not common semiconductor industry practices and represented an unnecessary risk. "Good enough" diodes could be made without developing these techniques. This is still the case for the DINS application, and these concepts are mentioned only to point out that we have not exhausted all possibilities. Someday, someone may need an even harder detector and he should consider these ideas.

Figure 6 is a microphotograph of the first generation DINS photodiode chip (#984, 1978). In this mosaic photo the semicircular structures are the photodiodes. Squares around the periphery of the chip are the fly-wire bonding pads, retangular structures with interleaved fingers are field effect transistors, (FET's) and S shaped structures are load resistors. Originally Harris intended to accomplish the first stage of amplification on the photodiode chip using JFET devices whose thickness is approximately the same as the photodiode. This idea eventually had to be discarded because the photocurrents in the JFET structures were large compared to those generated in these rad hard diodes or in vertical bipolar transistors, which are thicker devices with smaller lateral dimensions. As can be seen in Figure 6 neither the resistor nor the JFET devices were pinned-out and consequently were not tested. In this photo the light-colored, granular, areas are sputtered aluminum. The dark featureless areas are AR coatings, and the

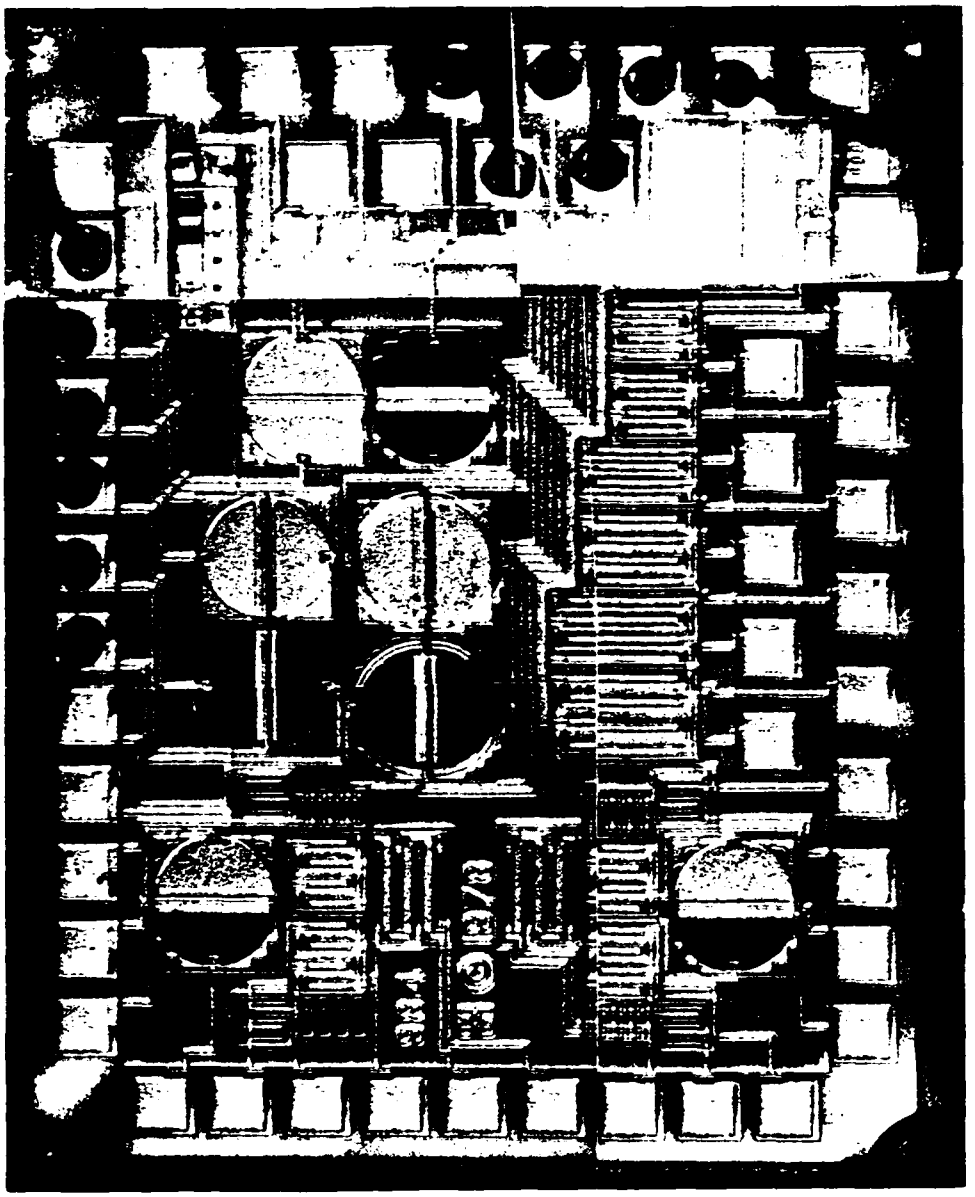

Figure 6. Microphotograph of Harris/DINS photodiode chip (~80X magnification) 1st generation #984, 1978.

gray featureless areas are passivating oxides. As a result of the July 1979 test series, Harris Semiconductor was requested to build a second test structure shown in microphotograph Figure 7 (chip #1061, 1979). On this second generation photodiode chip, only four load resistors and four photodiodes were constructed and/or pinned out. Harris made 4 variations on the same theme. All devices fabricated from slice #7 had received the phosphorous diffusion described in step 2 of Figure 4, and are referred to as buried-layer devices. All devices from wafer #13 had not received the phosphorous diffusion and, therefore, the bulk of the photodiode was of uniform 3-6 cm resistivity. All devices of Type I had one diode pair which was sensitive to optical radiation (sighted) and another diode pair which had been covered with aluminum (blind). Figure 7 shows such a structure. All chips of type II had four identical diodes (no blind diodes). A type II device is shown in Figure 8. All of the resistors on type I DINS chips had an aluminum over layer shown in more detail in Figure 9A. Resistors on Type II chips were not over coated with aluminum as shown in Figure 9b.

5. TEST AND RESULTS

In this section we describe the results of some electrical, optical and ionizing radiation tests.

The purpose of the electrical tests was to determine whether the individual devices had the correct characteristics. Electrically all of the diodes and resistors checked (about 200 each) were exactly as reported. The optical tests, were to determine the optical photocurrent response matching of both the resistors and photodiodes. This will be described in greater detail in the following paragraphs. Finally a rudimentary special response measurement was made on a limited number (about 60) of the photodiodes.

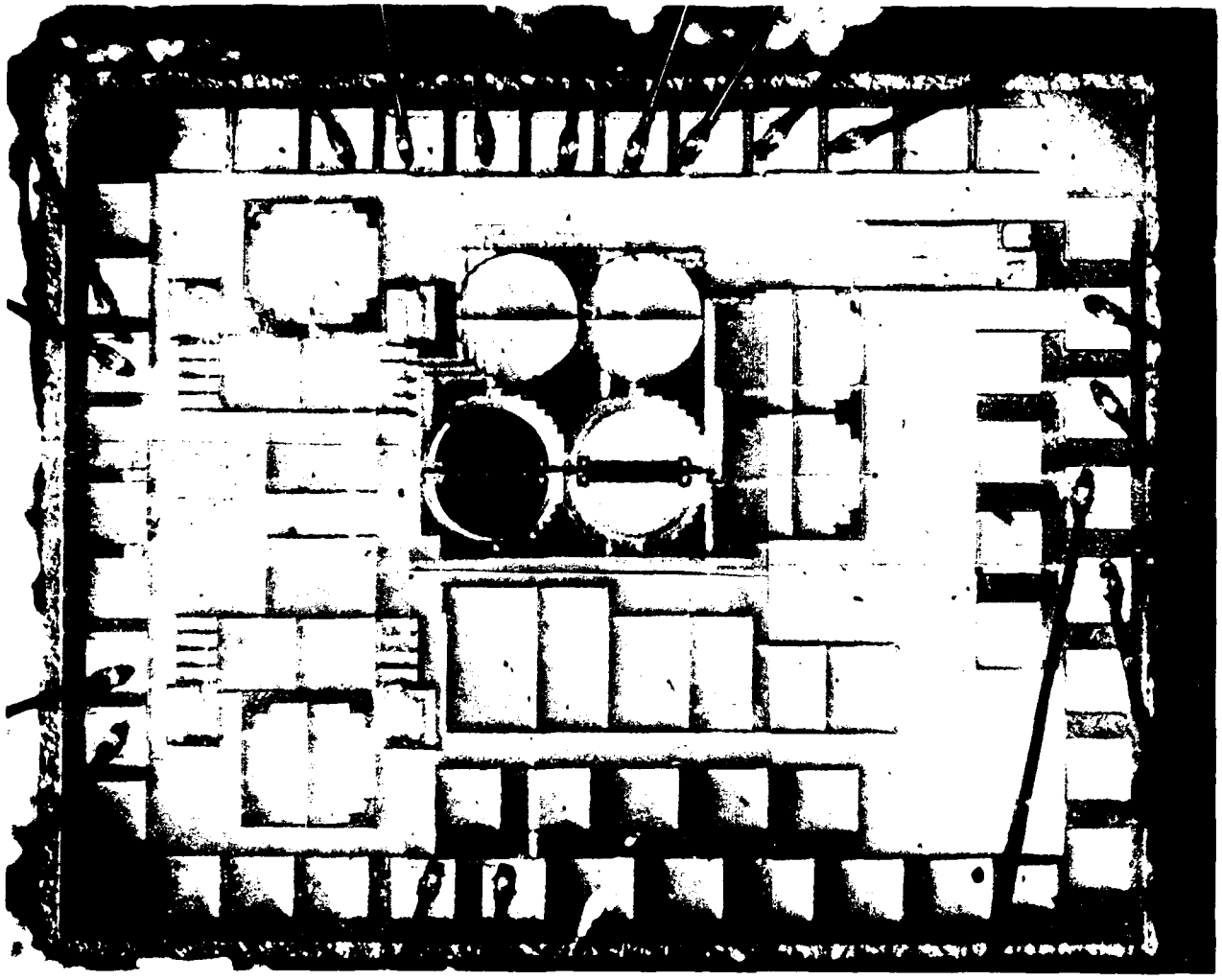

Figure 7. Second generation Harris/DINS photodiode (mosaic picture, 80X magnification) slice 13, style 1, 6/7/80.

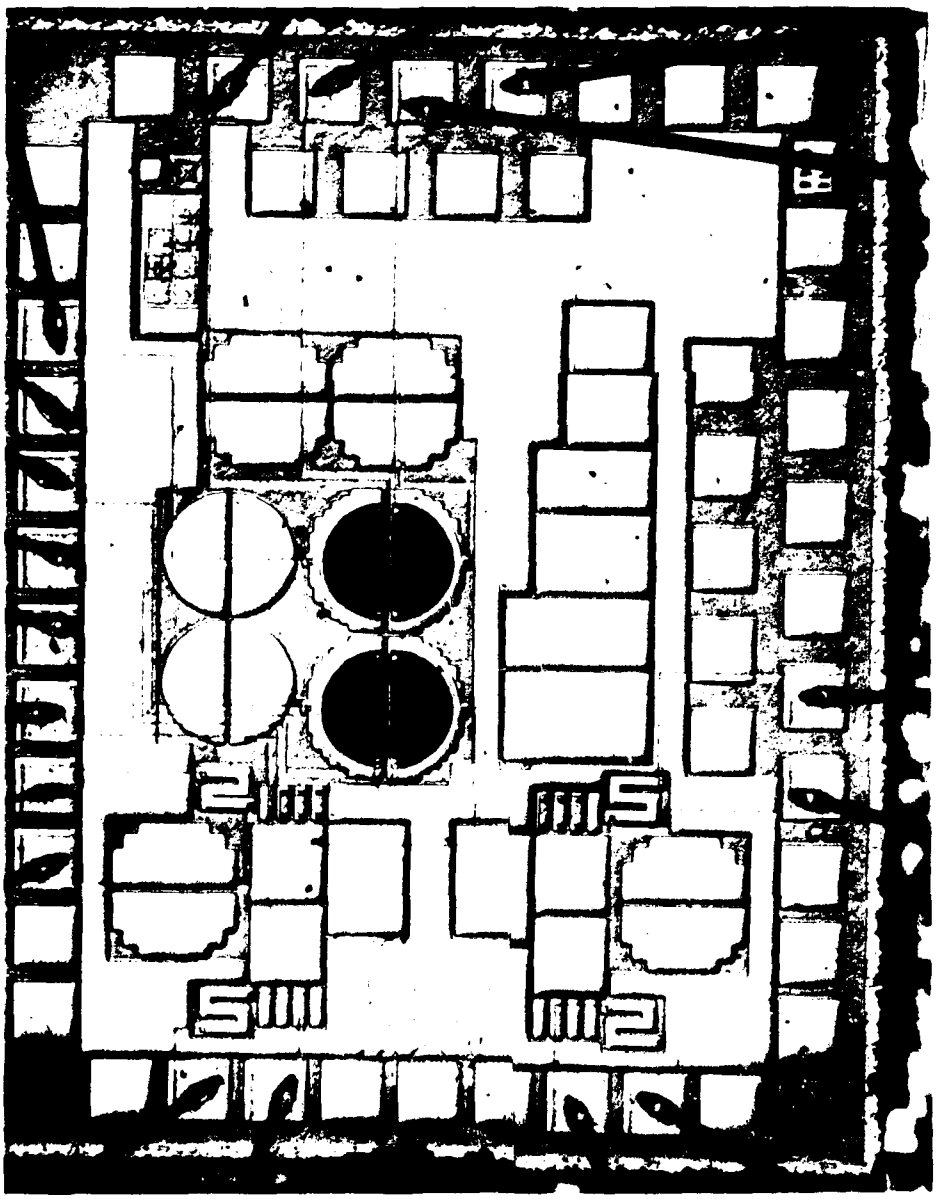

Figure 8. Second generation Harris/DINS photodiode with resistors (mosaic, 80x magnification) slice 13, style 2, 5/7/80.

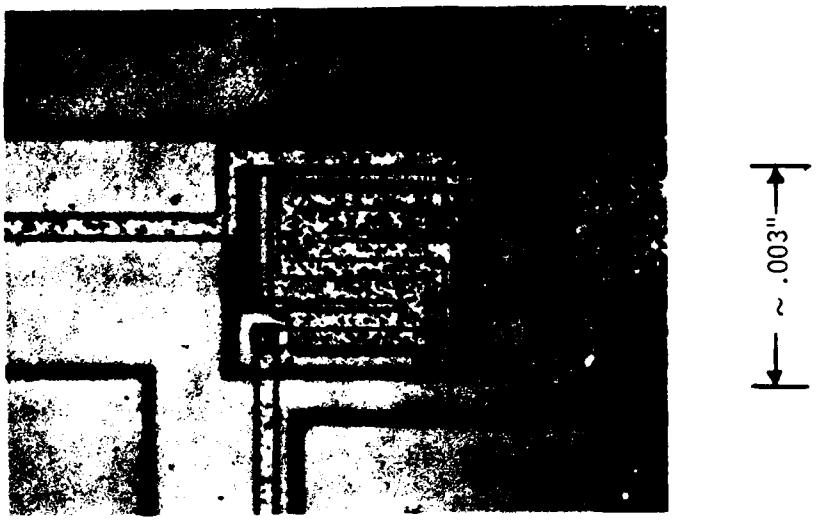

Figure 9a. Microphotograph at about 500X of the dielectrically isolated, ion implanted, 30 kΩ load resistor on a type I (slice 7) chip. Note the aluminum cover.

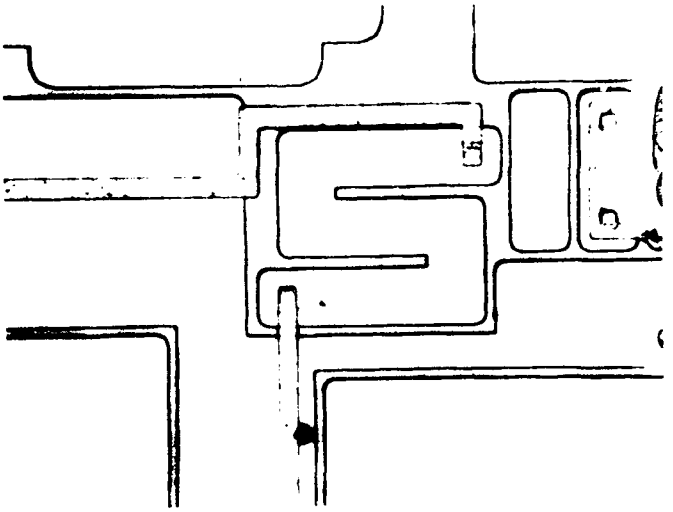

Figure 9b. Microphotograph at about 500X of the same load resistor without the aluminum cover (slice 7, type II).

5.1 METHOD

Before the ionizing radiation test the transient response of the photodiodes and load resistors was checked using a Vivitar Model 225 high pressure zenon photo flash. This confirmed that both the resistors and photodiodes exhibited some photocurrent response, however, the zenon flash evidently contained so much infra red radiation that the sighted and blind photodiodes responded nearly identically. This check served its primary purpose which was to confirm that the chip was correctly wired and biased, in preparation for the ionizing radiation tests.

The optical response characterization was something of an improvisation since there was neither time nor funding to perform an in-depth study. A Kodak model 750H 35 mm carousel slide projector was used to measure the spectral responsitivity and optical photocurrent matching of additional photodiode chips. The Kodak 750H has a 250 watt tungston halogen lamp with reflector, a cold mirror, and heat absorbing glass prior to the projector lens. The projected light was further concentrated with an F/1 convex lens. Approximately monochromatic light was created by projecting light through color transparencies. The spectral transmission characteristics of these transparencies is given in Figure 10. The intensity of the light appeared to be uniform with 10 percent across the center 75 percent of the beam. Most of the optical measurements were taken with an irradiance of from 0.01 to 0.1 watts/cm^2. An Optical Coating Laboratories Inc. (OCLI) model 51 PL solar cell was used as a "standard" comparison detector. This is a common off-the-shelf detector whose spectral response is approximately known. To define the illuminated area and reduce the photocurrent from the OCLI photo cell which is ½ x 1 cm it was placed behind an aluminum sheet with a 0.029 inch pin hole. Using this technique the photocurrents from the Harris DINS photodiodes could be directly compared to the photocurrent from the OCLI solar cell when exposed to white light or any one of 6 color filtered beams, both the Harris and OCLI photo detectors were reverse biased at 9 volts. The results of optical photo-

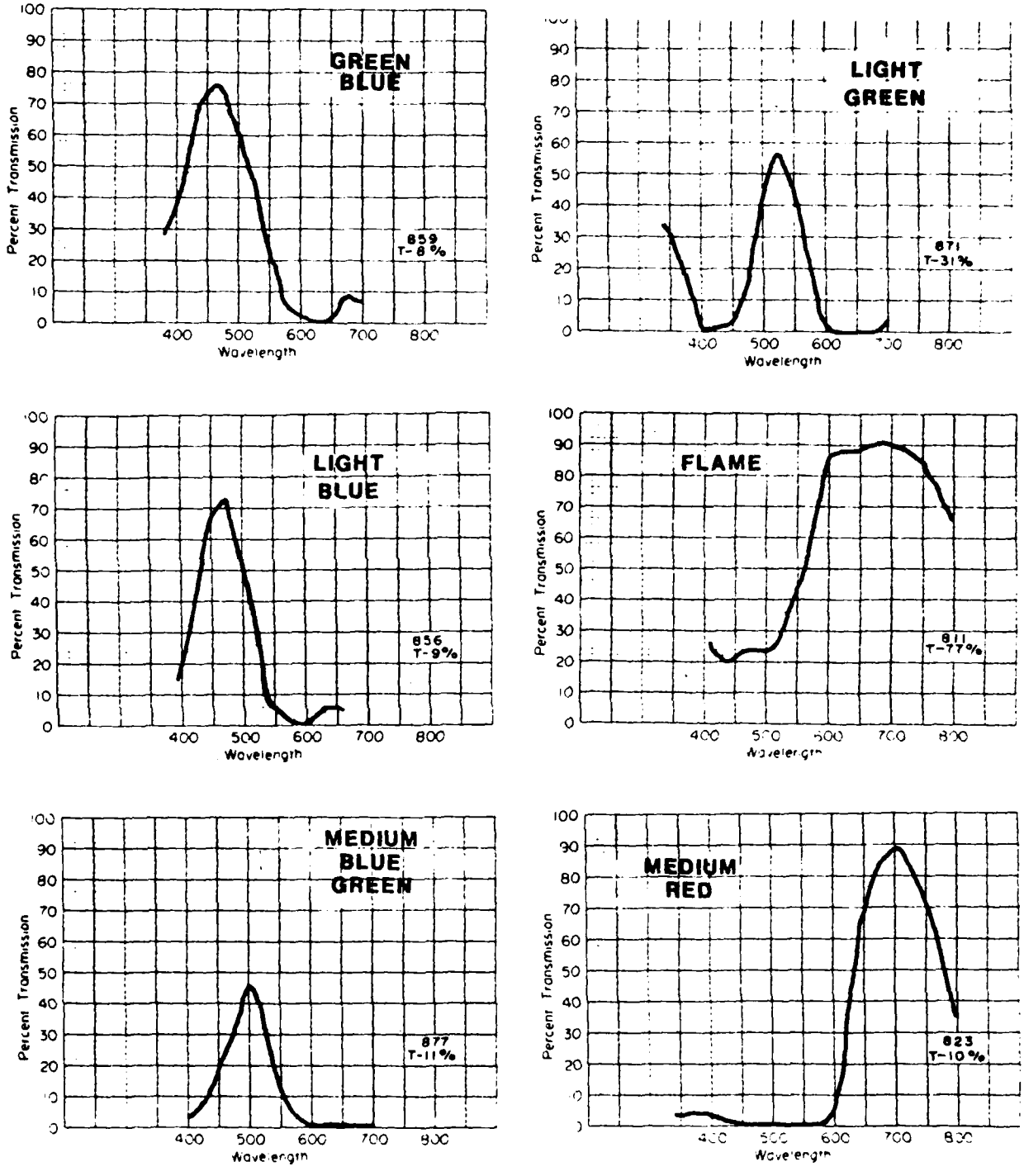

Figure 10. Spectral transmission measurements of selected optical filters.

current matching tests are indicated in Table 1. On the average, all photodiodes on any given clip produced photocurrents which matched to approximately 1.5 ± 0.5 percent, for nominally identical illuminization. This author is not prepared to certify that the illuminization was more uniform than 1 percent over the time or space required for the measurements.

The results of the spectral response measurements are indicated in Figure 11. This data was obtained by ratioing the measured photocurrent from the DINS diodes and OCLI solar cell (scaled for the different illuminated areas). Figure 12 shows the raw data for 8 different photo cells, two each of the four variations, representing unirradiated cells and cells which had been exposed to one megarad of 10 MeV electron radiation.

Although there is insufficient data for significant statistics it appears that the responsitivity of the irradiated cells is no less than 75 percent of the unradiated cells. The absolute magnitude of responsivity appears to vary by approximately ± 30 percent from chip to chip.

The response of the Harris photodiodes is very nearly what one would expect. The responsivity is on the average somewhat better than the OCLI solar cell at wave lengths below approximately 0.7 microns, probably because the Harris photo cells have an AR coating and the OCLI cell does not. The spectral response of the Harris photo cells decreases rapidly compared to the OCLI solar cell for wave lengths greater than 0.7 microns. This is almost certainly because the optical absorption coefficient decreases rapidly with increasing wave lengths (see Figure 2) which means that fewer carriers per photon are generated in the 5 micron thick Harris photo detectors than in the 130 μm thick OCLI cell. These data indicate that the Harris/DINS photodiodes have a responsivity of approximately 0.4 ± 0.1 amps/watt at 0.6328 microns. This means that, within the uncertainty of these measurements, Harris met their design goals.

TABLE 1. SUMMARY OF PHOTODIODE TESTING

SAMPLE ID	EXPOSURE ORDER	$x10^{-13}$ $\frac{coul}{rad}$	OPTICAL PHOTOCURRENT MATCH %	RADIATION PHOTOCURENT MATCH %	EXPOSURE K rads
7 I 1	1	5.7 ± 0.5	0.8 ± 0.3	~ 4.0	50
7 I 2	5	7.3	1.3	15 ± 5	120
7 I 3	9	5.9	0.6 ± 0.2	3-5	200
7 I 4	13	7.0 ± 0.5	4 ± 1	1-10	85
7 II 1	2	7.0 ± 0.7	0.7	0.4	330
7 II 2	6	7.0 ± 0.3	1.0 ± 0.3	2 to 10	80
7 II 3	10	5.6 ± 0.2	2.0 ± 0.3	2 to 7	130
7 II 4	14	7.6	2.1 ± 0.2	~ 10	30
13 I 1	3	3.6 ± 0.1	3 ± 2	3 ± 1	250
13 I 2	7	3.6 ± 0.4	0.4 ± 0.3	6 ± 4	50
13 I 3	11	8.5 ± 0.5	0.2	10 ± 5	200
13 I 4	15	3.5	0.9 ± 0.9	1 & 10	90
13 II 1	4	3.8	0.8 ± 0.2	6 ± 2	220
13 II 2	8	3.4 ± 0.3	1.0	~ 10	200
13 II 3	12	7.0 ± 0.3	1.0 ± 0.2	7 ± 1	70
13 II 4	16	---	1.6 ± 0.2	---	0
AVERAGE		5.77 ± 1.8	1.5 ± 0.5	6 ± 5	

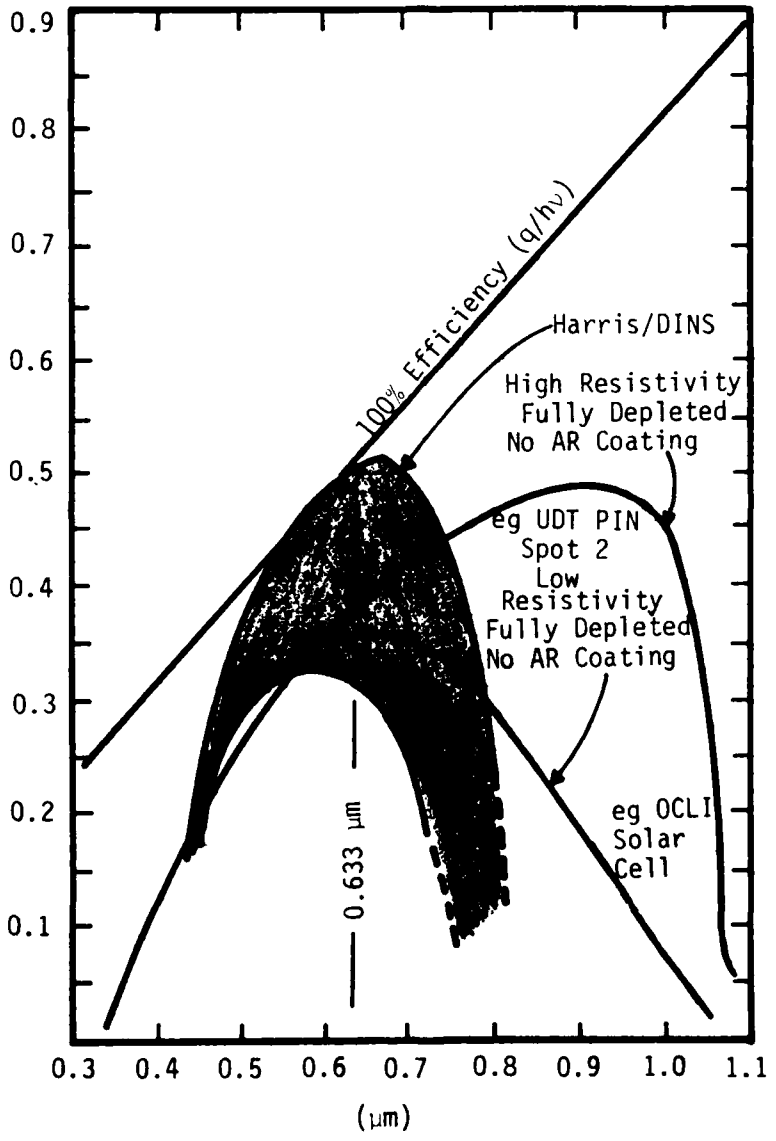

Figure 11. Spectral response of a perfect silicon photodetector, a high quality silicon photodetector, a typical solar cell and the Harris/DINS photodetectors. The DINS detectors response varied by ~ ±30% from chip to chip.

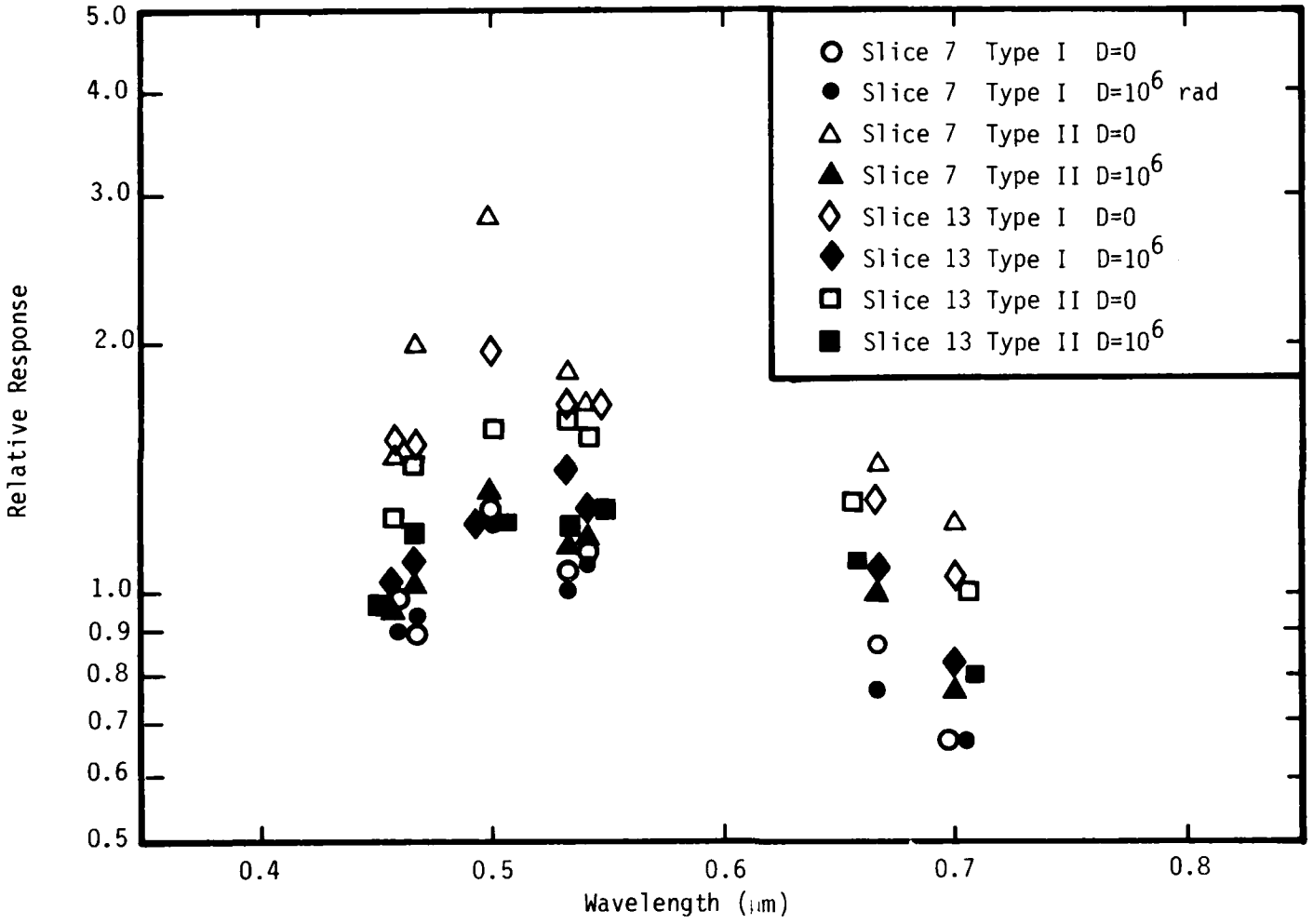

Figure 12. Optical photocurrent of four types of DINS diodes, ratioed to the current from an equal area of the OCLI solar cell. Comparing the irradiated cells with new ones indicates post irradiation responsivities of: 7I=97±7%, 7II=61±9%, 13I=76±8% and 13II=80±5%.

5.2 RADIATION TESTS

The purpose of these ionizating radiation tests was to measure the (1) total current generation constant and (2) photocurrent matching, for nominally identical photodiodes. Based on geometry and physics we expected a generation constant $Q/D = 7.8 \times 10^{-13}$ coul/rad. As a result of this test we measured $Q/D = 5.7 \pm 1.8 \times 10^{-13}$ coul/rad for (60 photodiodes).

5.3 EXPERIMENT DESCRIPTION

This test was conducted at the IRT Electron Linear Accelerator (linac) operated at 10 MeV, with a 100 ns pulse width, delivering approximately 800 rads per pulse ($\dot{D}$ approximately = 8×10^{9} rads/s). The results of this test are somewhat less precise than hoped for, because the linac performance was below par, due to an inoperative second section. This resulted in comparitively poor pulse-to-pulse reproducibility and an uncertain beam profile at the sample. Figure 13 schematically indicates the experimental configuration. Photodiodes and load resistors were biased with a nine volt battery. The integrated photocurrent for each pulse was measured by Tektronics 7844 & 556 oscilloscopes as shown, using the RC time constant established by the scope input impedence and cable capacidence. Cable capacidence was measured to be 2.71 nF, and since the oscilloscopes were operated in parallel, and input impedence for each scope plug-in was 1 MΩ the effective resistance was 500 KΩ (RC ≈ 1.35 ms). The oscilloscope plug-ins were calibrated immediately prior to use.

The dose at the sample location, for any particular linac pulse, was inferred from the output of a secondary emission monitor (SEM). The secondary emission monitor is a thin metal foil inside the beam tube, in front of the collimator and scatterer. Prior to sample irradiation, a calibrated thermister/wheatstone bridge dosimeter was used to measure the dose at the sample location while simultaneously monitoring the integrated output of the secondary emission monitor. The thermister calibration was

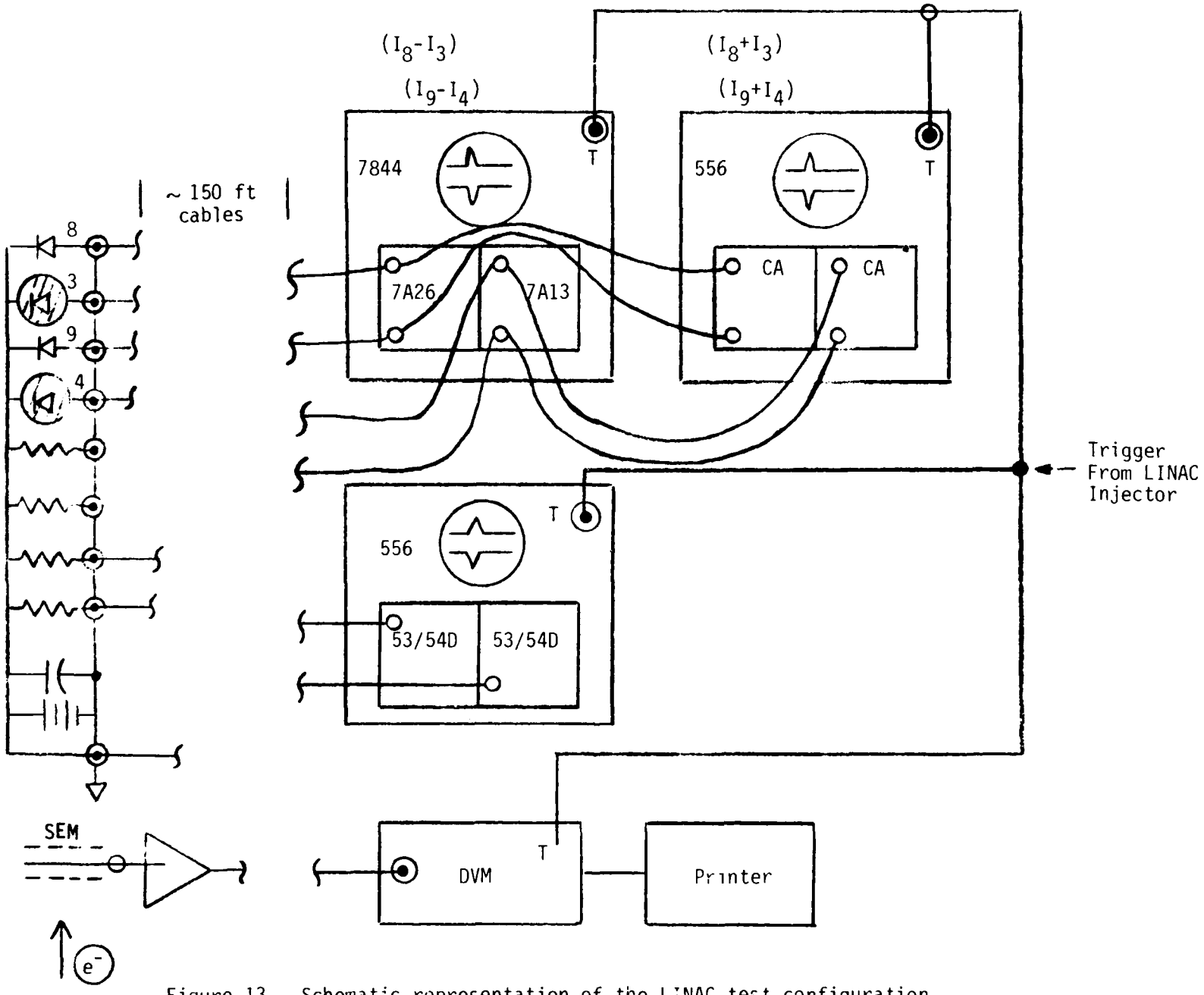

Figure 13. Schematic representation of the LINAC test configuration.

3.82 rads per microvolt. The dose/SEM reading calibration was 374 ± 25 rads per volt. The SEM readings were recorded automatically and printed on paper tape. Each sample was exposed to from 100 to 300 pulses, with data to measure $\Delta I/I$ and Q/D recorded on the first, last and at several intermediate pulses. To support the SEM based dosimetry, Far West radiochromic film dosimeters were attached to each sample. In addition to the sample group which was actively monitored during the test (15 chips), three each, of the four different type devices, were exposed passively, and in a biased condition, to 3 different total doses approximately 100 K rad, 300 K rad and 1 M rad (a total of 72 chips). The accuracy of the Far West dosimeters is estimated to be approximately ± 5 percent at 10^6 rads, approximately ± 10 percent at 10^5 rads, and approximately ± 20 percent below 10^5 rads. This uncertainty is principally a reading error.

5.4 RESULTS

The results of the linac tests were also summarized in Table 1. The measured radiation photocurrent for 60 photodiodes was $5.7 \pm 1.8 \times 10^{-13}$ coul/rad. Estimated experimental uncertainty is approximately ± 20 percent. The primary experimental uncertainty is the assessment of the dose, at the sample location, as inferred from the SEM reading. For diodes on any given chip a diode-to-diode variation photocurrent of approximately 5 percent is inferred from the radiation measurements. The uncertainty in this measurement is unknown and is related to the uniformity of the electron beam at the sample location. Variations in Q/D of as much as a factor of 2 were observed from chip to chip. It is not possible to separate real chip-to-chip response variations from pulse-to-pulse variations in the linac performance.

In the preceeding tests, of generation 1 photodiodes, we noted several examples of relative photocurrent response changing as a function of total accumulated dose. Such behavior was noted only once in this test of 15 chips (or 60 diodes), however, since these particular photodiodes

Part #13I-4 matched to within 1 percent both before and after irradiation, relative changes in response are of negligable significance.

The optically induced photocurrents in the load resistors were found to agree from unit to unit to approximately 4 ± 2 percent. We were not able to make satisfactory Q/D measurements at the linear accelerator. We suspect that we exceeded the common mode rejection ratio capacity of our oscilloscope.

5.5 SUMMARY

This second generation of Harris/Dins photodiodes is much improved over the first generation. The spectral response, $R(\lambda)$ (0.4 ± 0.1 amp/watt at 632.8 μm), and the radiation induced photocurrent, Q/D ($5.7 \pm 1.8 \times 10^{-13}$ coul/rad), are also quite reasonable (based on the reported geometry). Based on a measurement of approximately 60 photodiodes photocurrents from matching diodes on any particular chip is identical to approximately 1.5 ± 0.5 percent by optical measuring techniques, and matched to approximately 6 ± 5 percent from ionization radiation measurements. Chip-to-chip variations in Q/D or $R(\lambda)$ appeared to be ± 30 percent. Moreover, using simple optical tests, chips can be hand selected for photocurrent matches better than 1 percent. Optical performance is still quite satisfactory after accumulated dose of 1×10^6 rads.

REFERENCES

1. Passenheim, B.C., et al., "Ring Laser Gyroscope", prepared for Defense Nuclear Agency. IRT 8177-010., December 27, 1977.

2. Passenheim, B.C. and C.E. Mallon, "Nuclear Radiation Vulnerability of Ring Laser Gyroscopes", SPIE 1978.

3. Kim, Mitchell, IEEE Trans. Nucl. Sci., NS-24, December 1977.

4. Harris Semiconductor, DINS Design Report. Contract No. DNA001-78-C-0356-P00001, October 19, 1979.

5. Jenkins, Francis A. and Harvey E. White, "Fundamentals of Optics", McGraw Hill Book Co. NY. 1957.

6. Wang, E.Y., F.T.S. Yu, V.L. Simms, H.W. Brandhorst, Jr., and J.D. Broder, "Optium Design of Antireflection Coating for Silicon Solar Cells," Conf. Rec. of the 10th IEEE Photovoltaic Specialist Conf., p. 168, 1973.

7. Schwartz, J.P., "Improved Silicon Solar Cell Antireflective Coatings," Conf. Rec. of the 8th IEEE Photovoltaic Specialist Conf., p. 173, 1970.

8. Musset, A., and A. Thelen, Progress in Optics (E. Wolf, ed.), Chapter 4., North-Holland, Amsterdam, 1970.

DISTRIBUTION LIST

DEPARTMENT OF DEFENSE

Assistant to the Secretary of Defense, Atomic Energy
ATTN: Executive Assistant

Command & Control Technical Center
ATTN: C-362, G. Adkins

Defense Advanced Rsch Proj Agency
ATTN: J. Fraser
ATTN: R. Reynolds

Defense Electronic Supply Center
ATTN: DEFC-ESA

Defense Logistics Agency
ATTN: DLA-SE
ATTN: DLA-QEL, J. Slattery

Defense Nuclear Agency
ATTN: RAEV (TREE)
4 cy ATTN: TITL

Defense Technical Information Center
12 cy ATTN: DD

Field Command
Defense Nuclear Agency
ATTN: FCPR

Field Command
Defense Nuclear Agency
Livermore Branch
ATTN: FCPRL

National Security Agency
ATTN: T. Brown
ATTN: G. Daily
ATTN: P. Deboy

NATO School (SHAPE)
ATTN: U.S. Documents Officer

Under Secretary of Defense for Rsch & Engrg
ATTN: Strategic & Space Sys (OS)

DEPARTMENT OF THE ARMY

BMD Advanced Technology Center
Department of the Army
ATTN: ATC-T
ATTN: ATC-O, F. Hoke

BMD Systems Command
Department of the Army
ATTN: BMDSC-HW, R. Dekalb

Deputy Chief of Staff for Rsch Dev & Acq
Department of the Army
ATTN: Advisor for RDA Analysis, M. Gale

U.S. Army Armament Rsch Dev & Cmd
ATTN: DRDAR-LCA-PD

U.S. Army Communications R&D Command
ATTN: D. Huewe

DEPARTMENT OF THE ARMY (Continued)

Harry Diamond Laboratories
Department of the Army
ATTN: DELHD-N-RBH, J. Halpin
ATTN: DELHD-N-P
ATTN: DELHD-N-RBC, J. McGarrity
ATTN: DELHD-N-RBH, H. Eisen
ATTN: DELHD-N-RBH

U.S. Army Material & Mechanics Rsch Ctr
ATTN: DRXMR-H, J. Hofmann

U.S. Army Missile Command
3 cy ATTN: RSIC

U.S. Army Nuclear & Chemical Agency
ATTN: Library

White Sands Missiles Range
Department of the Army
ATTN: STEWS-TE-AN, M. Squires
ATTN: STEWS-TE-AN, T. Leura

DEPARTMENT OF THE NAVY

Naval Air Systems Command
ATTN: AIR 350F

Naval Electronic Systems Command
ATTN: Code 5045.11, C. Suman

Naval Ocean Systems Center
ATTN: Code 4471

Naval Postgraduate School
ATTN: Code 1424, Library

Naval Research Laboratory
ATTN: Code 6816, D. Patterson
ATTN: Code 6600, J. McEllinney
ATTN: Code 5213, J. Killiany
ATTN: Code 6816, H. Hughes
ATTN: Code 6627, C. Guenzer
ATTN: Code 6601, A. Wolicki

Naval Sea Systems Command
ATTN: SEA-06J, R. Lane

Naval Surface Weapons Center
ATTN: Code F31
ATTN: Code F30

Naval Weapons Center
ATTN: Code 233

Naval Weapons Evaluation Facility
ATTN: Code AT-6

Naval Weapons Support Center
ATTN: Code 7024, J. Ramsey
ATTN: Code 7024, T. Ellis
ATTN: Code 70242, J. Munarin

Office of the Chief of Naval Operations
ATTN: OP 985F

DEPARTMENT OF THE NAVY (Continued)

Office of Naval Research
ATTN: Code 427, L. Cooper
ATTN: Code 220, D. Lewis

Strategic Systems Project Office
ATTN: NSP-2015
ATTN: NSP-27331, P. Spector
ATTN: NSP-2701, J. Pitsenberger
ATTN: NSP-230, D. Gold

DEPARTMENT OF THE AIR FORCE

Air Force Aeronautical Lab
ATTN: LPO, R. Hickmott
ATTN: LTE

Air Force Geophysics Laboratory
ATTN: SULL
ATTN: SULL S-29

Air Force Institute of Technology
ATTN: ENP, J. Bridgeman

Air Force Systems Command
ATTN: XRLA
ATTN: DLW
ATTN: DLCA
ATTN: DLCAM

Air Force Technical Applications Ctr
ATTN: TAE

Air Force Weapons Laboratory
Air Force Systems Command
ATTN: NTYC, Mullis
ATTN: NTYC, Capt Swenson
3 cy ATTN: NTYC

Air Force Wright Aeronautical Lab
ATTN: POD, P. Stover

Air Force Wright Aeronautical Lab
ATTN: TEA, R. Conklin
ATTN: DHE

Air Logistics Command
Department of the Air Force
ATTN: OO-ALC/MM
ATTN: MMETH
ATTN: MMEDD

Assistant Chief of Staff
Studies & Analyses
Department of the Air Force
ATTN: AF/SAMI

Ballistic Missile Office
Air Force Systems Command
ATTN: ENSN, H. Ward

Ballistic Missile Office
Air Force Systems Command
ATTN: ENSN, J. Tucker
ATTN: SYDT
ATTN: ENMG
ATTN: ENBE

DEPARTMENT OF THE AIR FORCE (Continued)

Foreign Technology Division
Air Force Systems Command
ATTN: TQTD, B. Ballard
ATTN: PDJV

Headquarters Space Division
Air Force Systems Command
ATTN: AQT, W. Blakney
ATTN: AQM

Headquarters Space Division
Air Force Systems Command
ATTN: SZJ, R. Davis

Rome Air Development Center
Air Force Systems Command
ATTN: RBRP, C. Lane

Rome Air Development Center
Air Force Systems Command
ATTN: ESE, A. Kahan
ATTN: ESR, P. Vail
ATTN: ESER, R. Buchanan
ATTN: ESR, W. Shedd
ATTN: ETS, R. Dolan

Strategic Air Command
Department of the Air Force
ATTN: XPFS, M. Carra

Tactical Air Command
Department of the Air Force
ATTN: XPG

DEPARTMENT OF ENERGY

Department of Energy
Albuquerque Operations Office
ATTN: WSSB

OTHER GOVERNMENT AGENCIES

Central Intelligence Agency
ATTN: OSWR/NED
ATTN: OSWR/STD/MTB, A. Padgett

Department of Commerce
National Bureau of Standards
ATTN: Sec Ofc for K. Galloway
ATTN: Sec Ofc for J. Humphreys
ATTN: Sec Ofc for J. French

NASA
Goddard Space Flight Center
ATTN. J. Adolphsen
ATTN: V. Danchenko

NASA
George C. Marshall Space Flight Center
ATTN: M. Nowakowski
ATTN: EGO2
ATTN: L. Haniter

NASA
ATTN: J. Murphy

OTHER GOVERNMENT AGENCIES (Continued)

NASA
Lewis Research Center
ATTN: M. Baddour

NASA
Ames Research Center
ATTN: G. Deyoung

DEPARTMENT OF ENERGY CONTRACTORS

Lawrence Livermore National Lab
ATTN: Tech Info Dept, Library

Los Alamos National Laboratory
ATTN: J. Freed

Sandia National Lab
ATTN: F. Coppage
ATTN: J. Hood
ATTN: J. Barnum
ATTN: R. Gregory
ATTN: W. Dawes

DEPARTMENT OF DEFENSE CONTRACTORS

Advanced Microdevices, Inc
ATTN: J. Schlageter

Advanced Research & Applications Corp
ATTN: R. Armistead
ATTN: L. Palcuti

Aerojet Electro-Systems Co
ATTN: D. Toomb

Aerospace Corp
ATTN: S. Bower
ATTN: R. Crolius
ATTN: D. Fresh

Aerospace Industries Assoc of America, Inc
ATTN: S. Siegel

Battelle Memorial Institute
ATTN: R. Thatcher

BDM Corp
ATTN: D. Wunch
ATTN: R. Pease
ATTN: D. Alexander

Bendix Corp
ATTN: E. Meeder

Boeing Co
ATTN: D. Egelkrout

Boeing Co
ATTN: I. Arimura
ATTN: W. Rumpza
ATTN: C. Rosenberg
ATTN: A. Johnston

Burr-Brown Research Corp
ATTN: H. Smith

Cincinnati Electronics Corp
ATTN: L. Hammond
ATTN: C. Stump

DEPARTMENT OF DEFENSE CONTRACTORS (Continued)

California Institute of Technology
ATTN: W. Price
ATTN: A. Stanley
ATTN: A. Shumka

Charles Stark Draper Lab, Inc
ATTN: Tech Library
ATTN: R. Ledger
ATTN: A. Freeman
ATTN: R. Bedingfield
ATTN: A. Schutz
ATTN: C. Lai
ATTN: P. Greiff

University of Denver
ATTN: F. Venditti

E-Systems, Inc
ATTN: K. Reis

Electronic Industries Association
ATTN: J. Hessman

EMM Corp
ATTN: F. Krch

Exp & Math Physics Consultants
ATTN: T. Jordan

Ford Aerospace & Communications Corp
ATTN: J. Davison
ATTN: Technical Information Services

Franklin Institute
ATTN: R. Thompson

Garrett Corp
ATTN: R. Weir

General Dynamics Corp
ATTN: W. Hansen

General Dynamics Corp
ATTN: O. Wood
ATTN: R. Fields

General Electric Co
ATTN: J. Andrews
ATTN: R. Casey
ATTN: J. Peden

General Electric Co
ATTN: J. Palchefsky, Jr
ATTN: W. Patterson
ATTN: Technical Library
ATTN: R. Benedict
ATTN: R. Casey

General Electric Co
ATTN: J. Reidl

General Electric Co
ATTN: R. Hellen

General Electric Co
ATTN: D. Cole
ATTN: J. Gibson

DEPARTMENT OF DEFENSE CONTRACTORS (Continued)

General Electric Co
ATTN: D. Pepin

General Research Corp
ATTN: Tech Info Ofc
ATTN: R. Hill

George C. Messenger, Consulting Eng
ATTN: G. Messenger

Georgia Institute of Technology
ATTN: R. Curry

Georgia Institute of Technology
ATTN: H. Denny

Goodyear Aerospace Corp
ATTN: Sec Control Station

Grumman Aerospace Corp
ATTN: J. Rogers

Harris Corporation
ATTN: J. Cornell
ATTN: C. Anderson
ATTN: T. Sanders

Honeywell, Inc
ATTN: R. Gumm

Honeywell, Inc
ATTN: C. Cerulli

Honeywell, Inc
ATTN: Tech Library

Hughes Aircraft Co
ATTN: J. Singletary
ATTN: R. McGowan

Hughes Aircraft Co
ATTN: W. Scott
ATTN: E. Smith
ATTN: A. Narevsky
ATTN: D. Shumake

IBM Corp
ATTN: H. Mathers
ATTN: T. Martin

IBM Corp
ATTN: F. Tietze

IIT Research Institute
ATTN: I. Mindel

Institute for Defense Analyses
ATTN: Tech Info Svcs

International Business Machine Corp
ATTN: J. Ziegler

International Tel & Tel Corp
ATTN: A. Richardson
ATTN: Dept 608

Intersil, Inc
ATTN: D. Macdonald

DEPARTMENT OF DEFENSE CONTRACTORS (Continued)

JAYCOR
ATTN: T. Flanagan
ATTN: L. Scott
ATTN: R. Stahl

Johns Hopkins University
ATTN: P. Partridge

Kaman Sciences Corp
ATTN: M. Bell
ATTN: N. Beauchamp
ATTN: J. Lubell

Kaman Tempo
ATTN: M. Espig
ATTN: DASIAC

Kaman Tempo
ATTN: DASIAC

Litton Systems, Inc
ATTN: J. Retzler

Lockheed Missiles & Space Co, Inc
ATTN: J. Crowley
ATTN: J. Smith

Lockheed Missiles & Space Co, Inc
ATTN: E. Smith
ATTN: C. Thompson
ATTN: D. Phillips
ATTN: M. Smith
ATTN: E. Hessee
ATTN: P. Bene

M.I.T. Lincoln Lab
ATTN: P. McKenzie

Magnavox Govt & Indus Electronics Co
ATTN: W. Richeson

Martin Marietta Corp
ATTN: H. Cates
ATTN: W. Brockett
ATTN: W. Janocko
ATTN: R. Gaynor
ATTN: S. Bennett

Martin Marietta Corp
ATTN: E. Carter

McDonnell Douglas Corp
ATTN: D. Dohm
ATTN: M. Stitch
ATTN: R. Kloster
ATTN: Library

McDonnell Douglas Corp
ATTN: J. Holmgrem
ATTN: D. Fitzgerald

McDonnell Douglas Corp
ATTN: Tech Lib

Mission Research Corp
ATTN: C. Longmire
5 cy ATTN: Document Control

Mission Research Corp
ATTN: R. Pease

DEPARTMENT OF DEFENSE CONTRACTORS (Continued)

Mission Research Corp, San Diego
ATTN: V. Van Lint
ATTN: J. Raymond
4 cy ATTN: B. Passenheim

Mission Research Corporation
ATTN: W. Ware

Mitre Corp
ATTN: M. Fitzgerald

Motorola, Inc
ATTN: A. Christensen

Motorola, Inc
ATTN: O. Edwards

National Academy of Sciences
ATTN: Nat Materials Advisory Bd
ATTN: R. Shane

National Semiconductor Corp
ATTN: R. Wang
ATTN: A. London

University of New Mexico
ATTN: H. Southward

Norden Systems, Inc
ATTN: Tech Lib
ATTN: D. Longo

Northrop Corp
ATTN: J. Srour

Northrop Corp
ATTN: L. Apodaca
ATTN: P. Gardner
ATTN: T. Jackson

Pacific-Sierra Research Corp
ATTN: H. Brode

Physics International Co
ATTN: J. Shea
ATTN: Division 6000

R & D Associates
ATTN: S. Rogers
ATTN: P. Haas

Rand Corp
ATTN: C. Crain

Raytheon Co
ATTN: J. Ciccio

Raytheon Co
ATTN: H. Flescher
ATTN: A. Van Doren

RCA Corp
ATTN: G. Brucker
ATTN: V. Mancino

RCA Corp
ATTN: D. O'Connor
ATTN: Ofc N103

DEPARTMENT OF DEFENSE CONTRACTORS (Continued)

RCA Corp
ATTN: R. Killion

RCA Corp
ATTN: W. Allen

Rensselaer Polytechnic Institute
ATTN: R. Gutmann

Research Triangle Institute
ATTN: Sec Ofc for M. Simons, Jr

Rockwell International Corp
ATTN: V. De Martino
ATTN: V. Strahan
ATTN: J. Brandford
ATTN: V. Michel

Rockwell International Corp
ATTN: T. Yates
ATTN: TIC BA08

Rockwell International Corp
ATTN: D. Vincent

Sanders Associates, Inc
ATTN: L. Brodeur

Science Applications, Inc
ATTN: D. Millward

Science Applications, Inc
ATTN: D. Long
ATTN: V. Ophan
ATTN: V. Verbinski
ATTN: J. Naber

Science Applications, Inc
ATTN: W. Chadsey

Science Applications, Inc
ATTN: D. Stribling

Singer Co
ATTN: J. Brinkman

Singer Co
ATTN: R. Spiegel

Sperry Rand Corp
ATTN: Engineering Lab

Sperry Rand Corp
ATTN: C. Craig
ATTN: P. Maraffino
ATTN: R. Viola
ATTN: F. Scaravaglione

Sperry Rand Corp
ATTN: D. Schow

Sperry UNIVAC
ATTN: J. Inda

Spire Corp
ATTN: R. Little

DEPARTMENT OF DEFENSE CONTRACTORS (Continued)

SRI International
ATTN: A. Whitson
ATTN: B. Gasten
ATTN: P. Dolan

Sylvania Systems Group
ATTN: C. Thornhill
ATTN: L. Blaisdell
ATTN: L. Pauples

Sylvania Systems Group
ATTN: J. Waldron
ATTN: P. Fredrickson
ATTN: H. Ullman
ATTN: H & V Group

Systron-Donner Corp
ATTN: J. Indelicato

Teledyne Ryan Aeronautical
ATTN: J. Rawlings

Texas Instruments, Inc
ATTN: R. Stehlin
ATTN: A. Peletier

Texas Instruments, Inc
ATTN: F. Poblenz

TRW Systems and Energy
ATTN: G. Spehar
ATTN: B. Gililland

DEPARTMENT OF DEFENSE CONTRACTORS (Continued)

TRW Defense & Space Sys Group
ATTN: O. Adams
ATTN: A. Pavelko
ATTN: H. Holloway
ATTN: P. Guilfoyle
ATTN: R. Kingsland
ATTN: A. Witteles

TRW Defense & Space Sys Group
ATTN: W. Willis
ATTN: F. Fay
ATTN: R. Kitter
ATTN: M. Gorman

Vought Corp
ATTN: R. Tomme
ATTN: Library
ATTN: Tech Data Center

Westinghouse Electric Co
ATTN: L. McPherson

Westinghouse Electric Corp
ATTN: H. Kalapaca
ATTN: D. Crichi

IRT Corp
ATTN: N. Rudie
ATTN: J. Harrity

END

DATE
FILMED

1-81

DTIC